ENVIRONMENTAL RESEARCH
LETTERS

LETTER

Five years of variability in the global carbon cycle: comparing an estimate from the Orbiting Carbon Observatory-2 and process-based models

Zichong Chen[1,*], Deborah N Huntzinger[2], Junjie Liu[3], Shilong Piao[4], Xuhui Wang[4], Stephen Sitch[5], Pierre Friedlingstein[6], Peter Anthoni[7], Almut Arneth[7], Vladislav Bastrikov[8], Daniel S Goll[9], Vanessa Haverd[10], Atul K Jain[11], Emilie Joetzjer[12], Etsushi Kato[13], Sebastian Lienert[14], Danica L Lombardozzi[15], Patrick C McGuire[16], Joe R Melton[17], Julia E M S Nabel[18], Julia Pongratz[18,19], Benjamin Poulter[20], Hanqin Tian[21], Andrew J Wiltshire[22], Sönke Zaehle[23] and Scot M Miller[1]

[1] Department of Environmental Health and Engineering, Johns Hopkins University, Baltimore, MD, United States of America
[2] School of Earth & Sustainability, Northern Arizona University, Flagstaff, AZ, United States of America
[3] Jet Propulsion Laboratory, California Institute of Technology, Pasadena, CA, United States of America
[4] Sino-French Institute for Earth System Science, College of Urban and Environmental Sciences, Peking University, Beijing, People's Republic of China
[5] College of Life and Environmental Sciences, University of Exeter, Exeter, United Kingdom
[6] College of Engineering, Mathematics and Physical Sciences, University of Exeter, Exeter, United Kingdom
[7] Karlsruhe Institute of Technology, Institute of Meteorology and Climate, Research/Atmospheric Environmental Research, 82467 Garmisch-Partenkirchen, Germany
[8] Laboratoire des Sciences du Climat et de l'Environnement, Institut Pierre-Simon Laplace, CEA-CNRS-UVSQ, CE Orme des Merisiers, 91191 Gif-sur-Yvette, CEDEX, France
[9] Lehrstuhl fur Physische Geographie mit Schwerpunkt Klimaforschung, Universität Augsburg, Augsburg, Germany
[10] CSIRO Oceans and Atmosphere, G.P.O. Box 1700, Canberra, ACT 2601, Australia
[11] Department of Atmospheric Sciences, University of Illinois, Urbana, IL, United States of America
[12] Centre National de Recherche Meteorologique, Unite mixte de recherche 3589 Meteo-France/CNRS, 42 Avenue Gaspard Coriolis, 31100 Toulouse, France
[13] Institute of Applied Energy (IAE), Minato-ku, Tokyo 105-0003, Japan
[14] Climate and Environmental Physics, Physics Institute and Oeschger Centre for Climate Change Research, University of Bern, Bern, Switzerland
[15] National Center for Atmospheric Research, Climate and Global Dynamics, Terrestrial Sciences Section, Boulder, CO, United States of America
[16] Department of Meteorology, Department of Geography & Environmental Science, National Centre for Atmospheric Science, University of Reading, Reading, United Kingdom
[17] Climate Research Division, Environment and Climate Change Canada, Victoria, BC, Canada
[18] Max Planck Institute for Meteorology, Hamburg, Germany
[19] Ludwig-Maximilians-Universität München, Luisenstr. 37, 80333 Munich, Germany
[20] NASA Goddard Space Flight Center, Biospheric Sciences Laboratory, Greenbelt, MD, United States of America
[21] International Center for Climate and Global Change Research, School of Forestry and Wildlife Sciences, Auburn University, 602 Ducan Drive, Auburn, AL, United States of America
[22] Met Office Hadley Centre, FitzRoy Road, Exeter EX1 3PB, United Kingdom
[23] Max Planck Institute for Biogeochemistry, P.O. Box 600164, Hans-Knöll-Str. 10, 07745 Jena, Germany
[*] Author to whom any correspondence should be addressed.

E-mail: zchen74@jhu.edu

Keywords: inter-annual variability, OCO-2 satellite, climate–carbon relationships, carbon cycle, environmental drivers

Supplementary material for this article is available online

OPEN ACCESS

RECEIVED
23 October 2020

REVISED
7 April 2021

ACCEPTED FOR PUBLICATION
22 April 2021

PUBLISHED
4 May 2021

Abstract

Year-to-year variability in CO_2 fluxes can yield insight into climate-carbon cycle relationships, a fundamental yet uncertain aspect of the terrestrial carbon cycle. In this study, we use global observations from NASA's Orbiting Carbon Observatory-2 (OCO-2) satellite for years 2015–2019 and a geostatistical inverse model to evaluate 5 years of interannual variability (IAV) in CO_2 fluxes and its relationships with environmental drivers. OCO-2 launched in late 2014, and we specifically evaluate IAV during the time period when OCO-2 observations are available. We then compare

inferences from OCO-2 with state-of-the-art process-based models (terrestrial biosphere model, TBMs). Results from OCO-2 suggest that the tropical grasslands biome (including grasslands, savanna, and agricultural lands within the tropics) makes contributions to global IAV during the 5 year study period that are comparable to tropical forests, a result that differs from a majority of TBMs. Furthermore, existing studies disagree on the environmental variables that drive IAV during this time period, and the analysis using OCO-2 suggests that both temperature and precipitation make comparable contributions. TBMs, by contrast, tend to estimate larger IAV during this time and usually estimate larger relative contributions from the extra-tropics. With that said, TBMs show little consensus on both the magnitude and the contributions of different regions to IAV. We further find that TBMs show a wide range of responses on the relationships of CO_2 fluxes with annual anomalies in temperature and precipitation, and these relationships across most of the TBMs have a larger magnitude than inferred from OCO-2. Overall, the findings of this study highlight large uncertainties in process-based estimates of IAV during recent years and provide an avenue for evaluating these processes against inferences from OCO-2.

1. Introduction

Interannual variability (IAV) in CO_2 fluxes is of critical importance in understanding the global carbon cycle. The magnitude of IAV in global terrestrial fluxes is large, comparable to that of land fluxes in an average year (Peylin *et al* 2013). An investigation of IAV also offers an opportunity to explore the sensitivity of the carbon cycle to changing environmental conditions and may therefore yield a better understanding of climate–carbon cycle relationships. Insight into contemporary IAV may therefore help inform projections of future CO_2 budgets under climate change (e.g. Cox *et al* 2013, Friedlingstein *et al* 2014, Hoffman *et al* 2014).

IAV in CO_2 fluxes at global scales is relatively well known; however, the contributions of different ecoregions to global IAV remain highly uncertain (e.g. Baker *et al* 2006, Peylin *et al* 2013, Deng *et al* 2014). *In situ* observations of atmospheric CO_2 have been extensively used to estimate global- and regional-scale IAV (e.g. Bousquet *et al* 2000, Gurney *et al* 2003, Rödenbeck *et al* 2003, Bruhwiler *et al* 2011, Peylin *et al* 2013, Shiga *et al* 2018, Hu *et al* 2019, Keppel-Aleks *et al* 2014). However, *in situ* measurement sites are unevenly distributed across the globe; therefore, inverse models using *in situ* observations are arguably not sensitive to CO_2 fluxes in undersampled regions like the tropics, where IAV is the largest (e.g. Baker *et al* 2006, Peylin *et al* 2013, Piao *et al* 2020). The advent of space-based observations of CO_2 provides greater coverage than *in situ* measurements and opens new window into the study of IAV, though these observations are available for a more limited time period (e.g. Houweling *et al* 2004, Chevallier *et al* 2007). For example, the Greenhouse Gases Observing Satellite (GOSAT), launched in 2009, is the first Earth-orbiting satellite that is designed to collect atmospheric CO_2 with sufficient accuracy to estimate surface CO_2 fluxes (Yokota *et al* 2009). Existing studies have leveraged GOSAT observations to estimate IAV (e.g. Guerlet *et al* 2013, Byrne *et al* 2019, 2020, Liu *et al* 2021). However, in a recent study, Byrne *et al* (2019) argued that current GOSAT observations can only be used to constrain IAV across continent-sized regions or larger spatial scales.

It is even more challenging to understand the relationships between IAV and underlying environmental drivers across different regions of the globe. Here we define 'environmental drivers' as meteorological variables or characteristics of the physical environment that may correlate with net ecosystem exchange (NEE) and can be quantified by measurements or models (e.g. precipitation, air temperature). Specifically, at small, local scales ($\sim$1 km^2), eddy flux tower measurements have been used as one of the most important approaches in quantifying IAV and its relationship with underlying environmental drivers (e.g. Baldocchi *et al* 2001, Barford *et al* 2001, Suyker *et al* 2001, Schwalm *et al* 2007, Jensen *et al* 2017). Due to the limited footprints of flux towers ($\sim$ 1 km^2), extrapolation of local eddy covariance measurements in space and time is necessary to obtain larger, regional- to global-scale estimate of CO_2 fluxes (e.g. Beer *et al* 2010, Jung *et al* 2011, Tramontana *et al* 2016). This upscaling can be challenging to do, and recent studies have argued that upscaling efforts tend to underestimate IAV relative to atmospheric inverse models (e.g. Byrne *et al* 2019, Jung *et al* 2020, Piao *et al* 2020). Furthermore, process-based terrestrial biosphere models (TBMs) have been widely used to simulate net carbon exchange (NEE) and IAV, and these models provide a means to attribute changes in net carbon uptake to specific environmental drivers (e.g. Tarnocai *et al* 2009, Medvigy *et al* 2010, Belshe *et al* 2013). With that said, TBMs do not show consensus on the magnitude of IAV in different ecoregions of the globe (e.g. Shiga *et al* 2018). Even when TBMs do agree on the magnitude of IAV, they often yield similar patterns for different reasons, i.e. TBMs display

very different sensitivities of IAV to environmental drivers (Piao *et al* 2013, Huntzinger *et al* 2017).

NASA's Orbiting Carbon Observatory 2 (OCO-2) satellite has the potential to provide additional, new information to investigate IAV and its relationships with environmental drivers (e.g. Eldering *et al* 2017). OCO-2 was launched in late 2014, so it does not provide as long of a record as many *in situ* or eddy flux measurement sites. With that said, its unprecedented global coverage and density of observations provides a new opportunity to examine IAV, albeit across a shorter window of time. Indeed, previous studies have used the global set of OCO-2 observations to estimate regional and global CO_2 fluxes (e.g. Chatterjee *et al* 2017, Liu *et al* 2017, Miller *et al* 2018, Chevallier *et al* 2019, Palmer *et al* 2019, Miller and Michalak 2020). For example, Liu *et al* (2017) and Chatterjee *et al* (2017) reported large tropical flux anomalies associated with warm and dry environmental conditions induced by the 2015–2016 El Niño from the terrestrial tropics and the tropical Pacific Ocean.

In this study, we employ OCO-2 observations (years 2015–2019) and a geostatistical inverse model (GIM) to examine the contributions of different regions to global IAV in CO_2 fluxes across the 5 year study period. We also explore the relationships between this IAV and anomalies in environmental drivers across the globe. We first present an overview of the GIM approach. We then present results on 5 years of IAV for different global biomes and evaluate the relationships between recent IAV and environmental drivers, followed by comparisons to an ensemble of 16 TBMs participating in the TRENDY dynamic global vegetation model project (e.g. Sitch *et al* 2015, Le Quéré *et al* 2018, Friedlingstein *et al* 2019, Piao *et al* 2020).

2. Methods

2.1. OCO-2 satellite observations

We use 10 s averages of bias-corrected total column CO_2 (XCO_2) generated from version 9 OCO-2 satellite observations. The 10 s averaged XCO_2 retrievals have previously been used in the OCO-2 inverse model inter-comparison project (e.g. Basu *et al* 2018, Chevallier *et al* 2019, Crowell *et al* 2019). Specifically, we include both land nadir and land glint retrievals in the model for years 2015 through 2019.

2.2. Geostatistical inverse model

We couple a GIM and a global adjoint model (version v35n of the GEOS-Chem adjoint, Henze *et al* 2007) to estimate five years of global CO_2 fluxes and associated uncertainties at a daily temporal resolution and a spatial resolution of 4° (latitude) by 5° (longitude). We define negative values of fluxes as net carbon uptake by the land, and positive values thus represent a net release from the land to the atmosphere. In this section, we provide an overview of the approach, and the supporting information text S1 (available online at stacks.iop.org/ERL/16/054041/mmedia) provides additional description of detailed model setup and specific equations.

In a GIM, we estimate surface fluxes that will best match atmospheric observations using an atmospheric transport model:

$$z = h(s) + \varepsilon \tag{1}$$

The fluxes s (dimensions $m \times 1$), when run through an atmospheric model, $h(\boldsymbol{s})$, should match the observations z (dimensions $n \times 1$) within a specific error ϵ (dimensions $n \times 1$).

A unique aspect of the GIM is that we can incorporate an array of environmental drivers to help describe the fluxes (s) instead of prescribing a traditional prior flux model. The GIM will scale the environmental drivers to best reproduce the atmospheric observations, and this component of fluxes is referred to as 'the deterministic model'. Furthermore, the GIM also estimates flux patterns that cannot be explained by the environmental drivers but are still evident in the atmospheric observations, and this component of fluxes is referred to as the 'stochastic component':

$$s = \mathbf{X}\beta + \zeta \tag{2}$$

where $\mathbf{X}$ is a matrix of environmental drivers (dimensions $m \times p$; see section 2.3), and the drift coefficients β (dimensions $p \times 1$) scale these environental drivers. Collectively, $\mathbf{X}\boldsymbol{\beta}$ is the 'determinstic model'. The unknown vector $\boldsymbol{\zeta}$ (dimensions $m \times 1$) is the stochastic component and is estimated at the model grid scale. The posterior flux estimate ($\widehat{\boldsymbol{s}}$, dimensions $m \times 1$) is a sum of the deterministic model ($\mathbf{X}\beta$) and the stochastic components ($\boldsymbol{\zeta}$).

We simultaneously estimate the fluxes ($\boldsymbol{s}$) and the coefficients (β) via minimizing the GIM cost function (e.g. Michalak *et al* 2004):

$$L_{s,\beta} = \frac{1}{2}(z - h(s))^T \mathbf{R}^{-1}(z - h(s)) + \frac{1}{2}(s - \mathbf{X}\beta)^T \mathbf{Q}^{-1}(s - \mathbf{X}\beta). \tag{3}$$

The cost function includes two covariance matrices; $\mathbf{R}$ (dimensions $n \times n$) and $\mathbf{Q}$ (dimensions $m \times m$). The covariance matrix $\mathbf{R}$ describes $\boldsymbol{z} - h(\boldsymbol{s})$, referred to here as the model-data mismatch errors. These errors include errors from the atmospheric measurements z and from the transport model $h()$. The covariance matrix $\mathbf{Q}$ prescribes the variances and spatiotemporal covariances of the stochastic component ($\boldsymbol{\zeta}$) and includes both diagonal and off-diagonal elements. supporting information text S1.1 describes the estimation of the covariance matrix parameters in detail.

In total, we assimilate five years of OCO-2 observations (i.e. $n = \sim 3.7 \times 10^5$) to estimate $\sim 6.0 \times 10^6$ unknown fluxes (m) at the model grid scale. We do

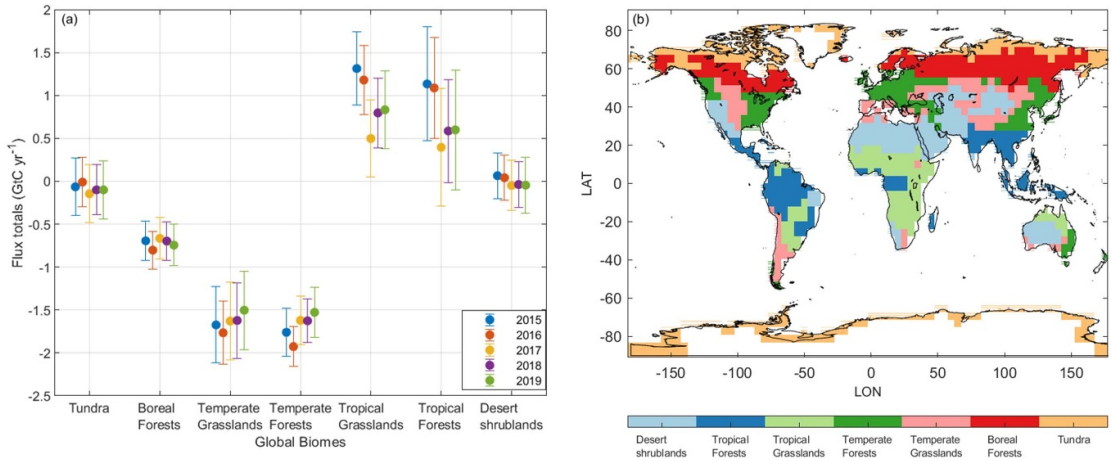

Figure 1. (a) Terrestrial biospheric flux totals for years 2015 through 2019 over the seven biomes, as estimated using OCO-2. Error bars indicate associated uncertainties with 95% confidence interval; (b) the seven biome-based regions aggregated from a world global map in Olson *et al* (2001). The flux totals shown here do not include flux patterns that map onto anthropogenic emissions from ODIAC but include all other components of the estimated fluxes. The estimate using OCO-2 suggests that tropical grasslands and tropical forests are large sources in years 2015 and 2016, and become smaller sources in years 2017 through 2019. Reproduced from Miller *et al* (2018). CC BY 4.0.

so by minimizing equation (3), a process described in the supporting information text S1. We also estimate the posterior uncertainties in the flux estimate ($\widehat{\boldsymbol{s}}$) using a reduced rank algorithm described in Saibaba and Kitanidis (2015) and Miller *et al* (2020), an approach described in detail in supporting information text S1.2.

We further compare the GIM flux estimates against aircraft-based observations of CO_2 and against CO_2 observations from the Total Carbon Column Observing Network (TCCON; Wunch *et al* 2011), as an external means to evaluate the inverse model estimates using OCO-2. supporting information text S7, figures S3–S10, and tables S3 and S4 display the details of these comparisons.

2.3. Model selection

We group the globe into seven biomes (figure 1(b)); for each biome, we consider an array of environmental drivers to include in the GIM (i.e. in **X**) available from NASA's Modern-Era Retrospective Analysis for Research and Applications, Version 2 (MERRA-2, Rienecker *et al* 2011). Specifically, these environmental drivers include daily 2 m air temperature, daily precipitation, 30 d average precipitation, photosynthetically active radiation (PAR), surface downwelling shortwave radiation, soil temperature at 10 cm depth, soil moisture at 10 cm depth, specific humidity, and relative humidity. We also include a non-linear function of air temperature (refer to hereafter as scaled temperature) from the Vegetation Photosynthesis and Respiration Model (Mahadevan *et al* 2008); in brief, this function characterizes the non-linear relationships between temperature and photosynthesis (e.g. Raich *et al* 1991). Note that we estimate a different coefficient (β) for each environmental driver in each biome and each year of the study period. Miller and Michalak (2020) argued that current OCO-2 observations are best-equipped to constrain terrestrial CO_2 fluxes for seven global biomes, and we therefore use seven biomes in this study.

We also incorporate additional fluxes in **X** that do not necessarily map onto any environmental drivers, including fossil fuel emissions from the Open-source Data Inventory for Anthropogenic CO_2 monthly fossil fuel emissions (ODIAC, Oda *et al* 2018), oceanic fluxes from the Estimating the Circulation and Climate of the Ocean consortium (ECCO-Darwin; Brix *et al* 2015, Carroll *et al* 2020), and biomass burning fluxes from Global Fire Emissions Database (GFED) version 4.1 (Giglio *et al* 2013). We find that the estimated coefficients (β) for ODIAC, ECCO-Darwin, and GFED are very uncertain if we attemp to constrain those coefficients (β) for each of these sources in each biome. Hence, we instead estimate a single coefficient for all three sources for the entire globe.

Furthermore, we include a constant column of ones in **X** for each biome and each year (including for the oceans). These columns help describe the mean behavior of the fluxes in each biome, and the environmental variables in **X** describe deviations from that mean behavior. All existing GIM studies to date include constant components within **X**, similar to the setup here (e.g. Gourdji *et al* 2008, 2012, Shiga *et al* 2018).

We utilize a model selection approach to objectively determine the optimal subset of environmental drivers that can best reproduce OCO-2 observations. We specifically employ a type of model selection known as the Bayesian Information Criterion (BIC), a commonly used statistical approach in regression analyses (e.g. Kass and Raftery 1995, Raftery 1995)

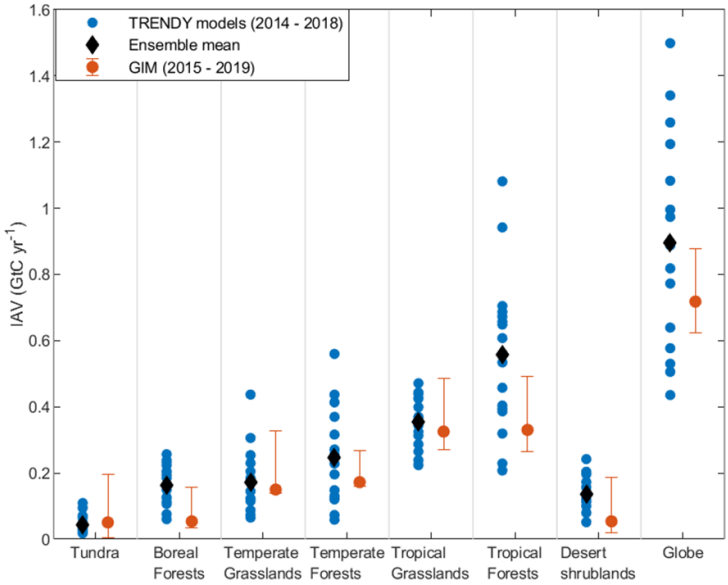

Figure 2. IAV during the 5 year study period from a suite of 16 TBMs in TRENDY (blue), from the ensemble mean of TBMs (black), and from the estimate using OCO-2 (red). Error bars indicate associated uncertainties (one standard deviation; see supporting information text S6). Most TBMs exhibit larger IAV compared to the estimate using OCO-2. Furthermore, a large number of TBMs (nine out of 16) estimate the largest IAV from tropical forests, whereas the findings using OCO-2 suggest that the tropical grasslands and tropical forests biomes make comparable contributions to global IAV, at least during the 5 year study period.

and inverse modelling studies (e.g. Gourdji *et al* 2012, Miller *et al* 2013, Fang and Michalak 2015, Miller *et al* 2016, 2018). In brief, the BIC rewards combinations of environmental drivers that better reproduce OCO-2 observations and penalizes combinations with too many environmental drivers to prevent overfitting; the best combination of environmental drivers is the combination with the lowest score. Miller *et al* (2018), Miller and Michalak (2020), and supporting information text S2 describes the specific setup for the BIC in greater detail.

2.4. State-of-the-art process-based models

We compare the inverse modeling estimates of IAV during the 5 year study period against an ensemble of 16 TBMs participating in TRENDY (v8; Sitch *et al* 2015, Friedlingstein *et al* 2019). Specifically, we collect net biospheric production (NBP) from TRENDY S3 simulations, which are forced over years 1901–2018 with changing CO_2, climate, and land use; NBP from TRENDY represents net CO_2 fluxes that take into account photosynthesis, plant and soil respiration, fire, land use change, and any carbon fluxes that are in and out of the ecosystem (*https://sites.exeter.acuk/trendy*). We compare against 5 years of model outputs from TRENDY to match the number of years in the inverse model. At the time of writing, TRENDY models are available through year 2018, so we use model outputs for years 2014–2018 (see table S1 for a full list of TBMs; Le Quéré *et al* 2018, Friedlingstein *et al* 2019, Piao *et al* 2020). Note that the climate forcing data used in TRENDY models are from Climatic Research Unit (CRU) and Japanese Reanalysis (JRA) datasets (CRUJRA; Harris *et al* 2014, Kobayashi *et al* 2015, Harris *et al* 2020).

3. Results and discussion

3.1. The contributions of different regions to global IAV during the study period

We find large differences in the magnitude of IAV (defined here as the standard deviation of annual flux totals) between the results from OCO-2 and the TBMs (figure 2). Most TBMs simulate larger IAV compared to the estimate using OCO-2 across the five-year study period. Furthermore, TBMs show little consensus on IAV across different biomes and the globe. With that said, the ensemble mean of these TBMs across different biomes and the globe are generally within the uncertainty bounds of IAV estimated using OCO-2, but numerous individual TBMs still fall outside the uncertainty bounds; this result implies that there is an opportunity to evaluate estimates of IAV within individual TBMs using current satellite observations of CO_2, at least during the time period for which satellite observations are available.

The estimate using OCO-2 further indicates that tropical biomes dominate global IAV and account for 87.8% of the variability during the 5 year study period. By contrast, most TBMs estimate a lower relative contribution (%) to global IAV from the tropics during this time, especially from the tropical grasslands biome (figure 3). Using OCO-2, we also

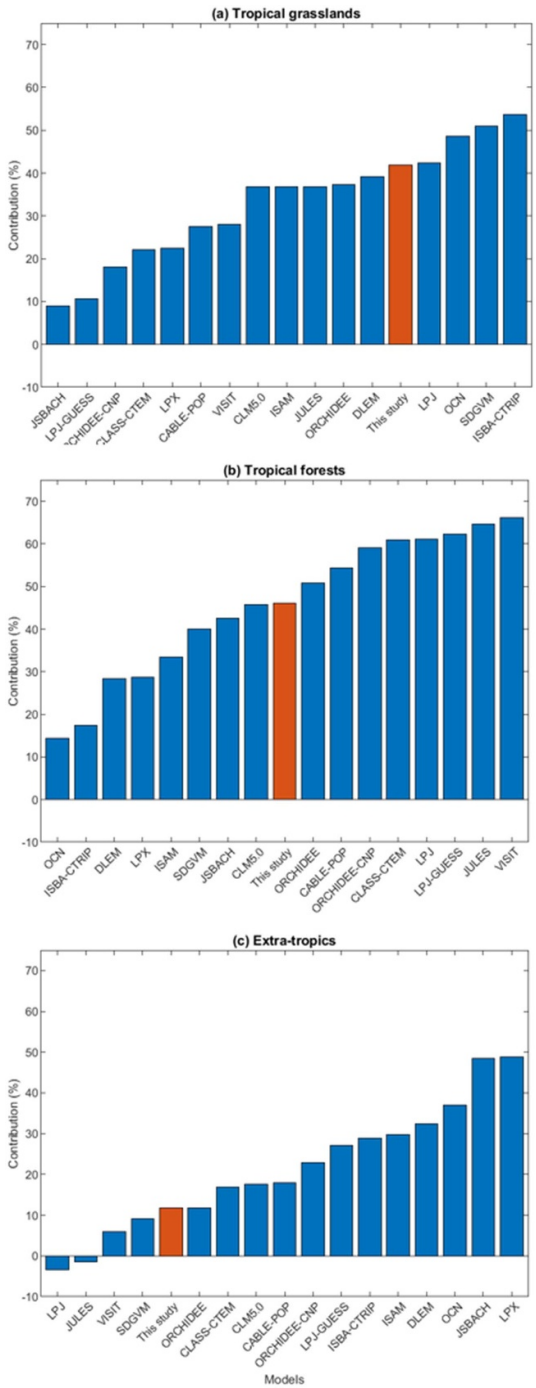

Figure 3. Relative contributions (%) of different biomes to global IAV, including (a) tropical grasslands, (b) tropical forests, and (c) the extra-tropics, from 16 TBMs (blue) and from the estimate using OCO-2 (red). In each panel, we order the models from the smallest contribution to the largest contribution. Compared to the estimate using OCO-2, most TBMs (12 out of 16) estimate lower relative contributions from tropical grasslands to global IAV during the study period, and approximately half of TBMs display lower relative contributions from tropical forests. By contrast, most TBMs suggest higher relative contributions from the extra-tropics to global IAV.

find large variations in the carbon cycle associated with the 2015–2016 El Niño and subsequent recovery; these perturbations dominate global IAV during 2015–2019 and account for the very large contribution of the tropics to IAV in the OCO-2 estimate (figures 1(a) and 2). Note that we estimate regional contributions (figure 3) to global IAV using a contribution framework developed by Ahlström *et al* (2015) (supporting information text S5); in brief, we weigh the flux anomaly (i.e. departure from a 5 year mean) from each individual region by its similarity to the global anomaly, and therefore enable a direct comparison of their relative importance to global IAV.

Specifically, the estimate using OCO-2 suggests that the tropical grasslands and tropical forests biomes make comparable contributions to global IAV during 2015–2019 (figure 3). Note here the tropical grasslands biome in Olson *et al* (2001; figure 1(b)) broadly encompasses grasslands, savanna, and agricultural land ecosystems (see figure 1 in Teluguntla *et al* 2015 or figure 16.1 in Thenkabail *et al* 2011) within the tropics. This finding differs from the TBMs, a majority of which (nine out of 16) estimate the largest contribution to global IAV from tropical forests (figure 3); a smaller number of TBMs (five out of 16) estimate the largest contribution from tropical grasslands.

Conversely, results from OCO-2 indicates that the extra-tropics accounts for a small fraction of recent, global IAV (12.2%). This result also disagrees with the estimates from the TBMs; most TBMs (12 out of 16) estimate larger IAV across the extra-tropics compared to the estimate using OCO-2 (figure 3). In fact, using OCO-2 we find a negative contribution from temperate grasslands to global IAV, which indicates the regional anomaly from temperate grasslands is in the opposite direction from the global anomaly. A previous study (Liu *et al* 2018) explored drought impact on CO_2 fluxes over the contiguous U.S. (CONUS), and suggested that the regional flux anomaly (departure from a 6 year mean) over the CONUS drought-impacted regions are in opposite directions of the global atmospheric CO_2 growth rate anomaly. The overall contribution of the extra-tropics is a sum of both positive and negative contributions of smaller-scale regions (e.g. Ahlström *et al* 2015). The negative contribution from temperate grasslands, therefore, acts to reduce the overall contributions of the extra-tropics to global IAV during years 2015–2019.

3.2. Connections between IAV during years 2015–2019 and environmental drivers

There is a growing consensus that tropical regions are the largest contributor to global IAV (e.g. Bousquet *et al* 2000, Peylin *et al* 2005, Gurney *et al* 2008, Jung *et al* 2017), but there is an ongoing debate over whether temperature or precipitation is a stronger correlate with this IAV in tropical regions (e.g. Zhao *et al* 2010, Wang *et al* 2014, Ahlström *et al* 2015, Jung *et al* 2017, Humphrey *et al* 2018). The findings using OCO-2 suggest that both environmental drivers play a key role in describing CO_2 variability across multiple scales—both in describing daily, grid-scale variability in CO_2 fluxes and in describing IAV, at

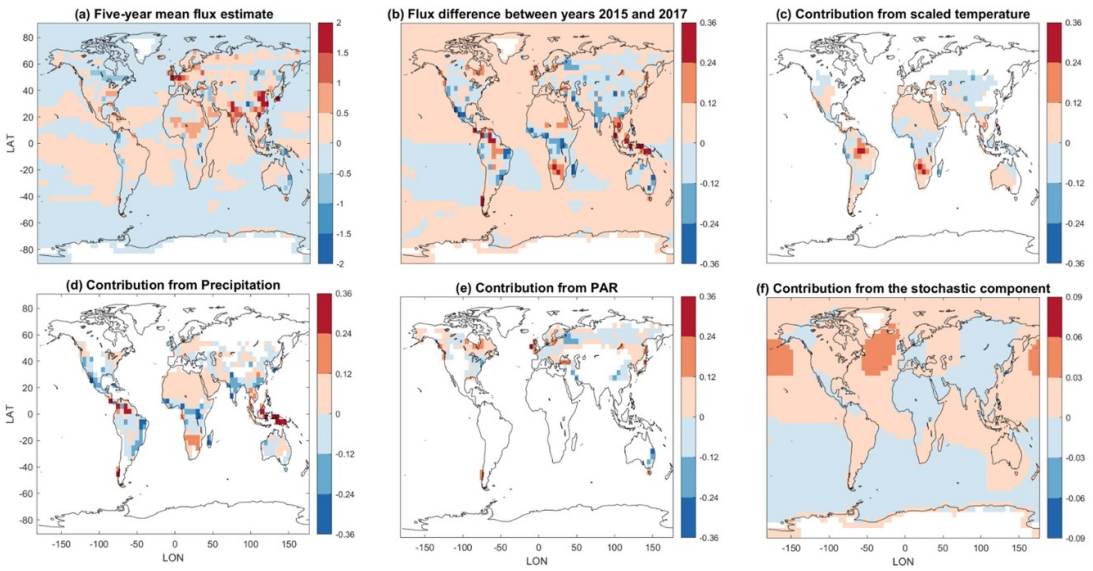

Figure 4. Five year mean flux estimate using OCO-2 (a; unit of μmol m^{-2} s^{-1}), and flux differences between years 2015 and 2017 (b); the flux estimate includes sources from NEE, fire, fossil fuel, and ocean in panels (a) and (b). Different environmental drivers in the deterministic model ($\mathbf{X}\beta$) contribute to these year-to-year differences, including air temperature (c), precipitation (d), PAR (e), and the stochastic component $\boldsymbol{\zeta}$ (f). The flux differences (b) over the tropics are mostly related to differences in air temperature (c) and precipitation (d) between the two years rather than from the stochastic component (f). The stochastic component here only reflects broad-scale flux differences. Note that the color bars used in panel (a), panels (b)–(e), and panel (f) are different. White colors in panels (c)–(e) reflect the fact that not all environmental drivers are selected in all biomes (see table S4).

least during the years when OCO-2 observations are available.

At the daily, model grid scale, a combination of temperature and precipitation can describe a substantial portion of the variability in CO_2 fluxes over the tropical grassland and tropical forest biomes (i.e. ∼78%–87% and ∼71%–83% of the flux variance across the study years, respectively). We define grid-scale variability as any spatiotemporal patterns in CO_2 fluxes that manifest at the resolutions of the GEOS-Chem model (daily, 4° (latitude) × 5° (longitude)) during the 5 year study period. Using the statistical model selection, we only select scaled temperature and precipitation in tropical biomes, further indicating the explanatory power of these environmental drivers. Figures 4(c)–(e) illustrate the sets of environmental drivers that are selected across individual biomes and their contributions to IAV in the inverse modeling estimate for years 2015–2019 (supporting information text S2, S3 and table S5 describe the full results of model selection for all biomes.).

An analysis of the 2015–2016 El Niño further illustrates the correlation between these environmental drivers and IAV in the posterior flux estimate across tropical regions. The 2015–2016 El Niño induced anomalously dry and warm environmental conditions in the tropics (e.g. Jiménez-Muñoz *et al* 2016) that altered global biospheric CO_2 fluxes (e.g. Liu *et al* 2017). We find that differences in temperature and precipitation in the deterministic component of the flux estimate ($\mathbf{X}\beta$, figures 4(c)–(e)) between years 2015 and 2017 contribute most to the grid-scale differences in CO_2 fluxes between the 2 years (figure 4(b)). By contrast, the stochastic component $\boldsymbol{\zeta}$ (figure 4(f)) describes relatively little year-to-year differences in the estimated fluxes. This result indicates that most year-to-year differences in the fluxes, as estimated using OCO-2, can be described by temperature and precipitation across tropical regions.

We also perform additional analysis to explore the impact of possible legacy effects, and disturbance (i.e. fire and land cover change) on IAV during the 5 year study period. We have limited ability in detecting legacy effects on IAV using five years of OCO-2 observations. Furthermore, fire and land cover change appear to play a small role in IAV for a 5 year period of this study. We discuss these topics in detail in supporting information text S3 and S4.

3.3. Relationships with environmental drivers help explain differences between OCO-2 and TBMs

To better understand the differences of estimated IAV between OCO-2 and the TBMs, we further examine the relationships between IAV and annual anomalies in key environmental drivers during the 5 year study period. We explicitly examine the relationships with annual anomalies in temperature and precipitation across the tropics, a region that makes the largest contributions to global IAV during this time period (figure 5).

We find that CO_2 fluxes in most TBMs tend to have stronger relationship with annual anomalies in

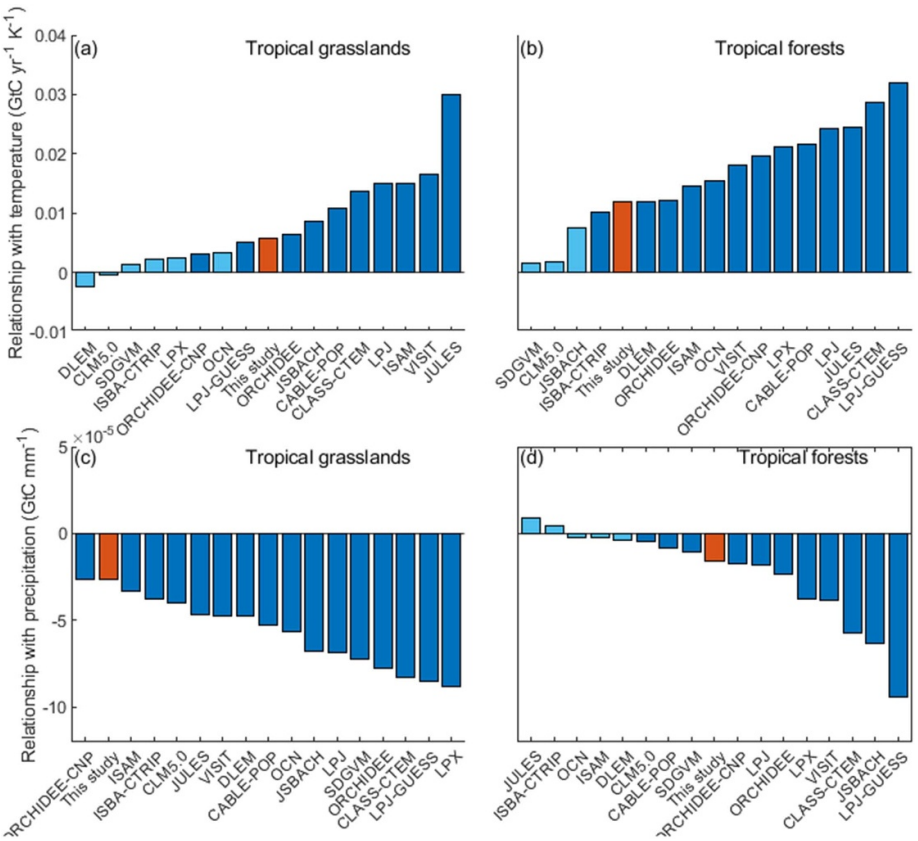

Figure 5. CO_2 fluxes in most TBMs (blue) show stronger relationships with annual anomalies in temperature and precipitation than inferred from OCO-2 (red) (a)–(d). This conclusion is particularly evident if we exclude models that show low correlation between anomalies in environmental drivers and flux anomalies ($R^2 < 0.1$), denoted in light blue above. In each panel, we order the models from the weakest relationship to the strongest relationship. For each TBM and the OCO-2 estimate, we fit a linear regression model between flux anomalies (departure from the 5 year mean) and annual anomalies in environmental drivers using model grid-scale datasets within each biome, and the slope of the linear regression model therefore indicates the relationships with the environmental drivers. Here we show the estimated slopes for various TBMs and OCO-2. Note the climate forcing data used in TRENDY models are from the CRUJRA datasets (see section 2.4), and we use environmental drivers from the CRUJRA data to examine the relationships here for these TBMs.

temperature and precipitation than estimated using OCO-2 (figure 5). This analysis likely helps to explain the differences of IAV between the TBMs and OCO-2. Indeed, TBMs that have stronger relationships with anomalies in temperature and precipitation relative to the estimate using OCO-2 tend to also display a larger magnitude of IAV over tropical biomes (figure 2).

Furthermore, some TBMs show different relationships with environmental drivers but still arrive at the same IAV. For example, VISIT shows strong relationship with temperature across tropical grasslands while LPX-Bern shows strong relationship with precipitation; however, estimated IAV over tropical grasslands between the two models are in close agreement. This finding further underscores the importance of rigorously characterizing drivers of IAV in TBMs, not just the magnitude of IAV. TBMs that describe very different relationships with temperature and precipitation would likely yield divergent projections of future carbon budgets under climate change (e.g. Huntzinger *et al* 2017).

4. Conclusions

In this study, we employ 5 years of OCO-2 satellite observations and a GIM to evaluate year-to-year variability in the global carbon cycle and its relationships with environmental drivers; we then compare IAV inferred from OCO-2 against 16 state-of-the-art TBMs.

This analysis provides an avenue for evaluating IAV in process-based flux estimates using satellite observations of CO_2. Despite the global observational coverage provided by OCO-2, the inverse modeling results presented here show substantial uncertainties (e.g. figure 2), pointing to the limitations of current space-based CO_2 monitoring. With that said, the uncertainties in inverse model are still smaller than the large range of estimates from the TBMs, implying that satellite observations can provide an important tool to evaluate IAV and even the environmental factors that correlate with this IAV. Furthermore, a longer record of satellite observations from

OCO-2 (or comparable instruments) in the future would facilitate an examination of longer time periods, and this study is a first step into exploring IAV using OCO-2 satellite observations.

Overall, we find that state-of-the-art TBMs show little consensus on the magnitude of IAV at either regional or global scales, at least for the 5 year period examined in this study. Compared to these models, our analysis using OCO-2 indicates (a) a larger contribution of tropical grasslands, savanna, and agricultural lands to global IAV during the study period, (b) a smaller contribution from the extra-tropics, and (c) a slightly smaller overall magnitude of IAV. These differences, particularly across the tropics, appear to stem from disagreement in the relationships within each model between carbon fluxes and annual anomalies in temperature and precipitation. This study hence reinforces the need to rigorously characterize the relationships between environmental drivers and IAV within TBMs, not just the estimated magnitude.

Data availability

Data information of the ObsPack data product is available at www.esrl.noaa.gov/gmd/ccgg/obspack/; data information of the TRENDY v8 is available at http://sites.exeter.acuk/trendy/.

The data that support the findings of this study are openly available at the following URL/DOI: ftp://ftp.cira.colostate.edu/ftp/BAKER/.

Acknowledgments

Financial support for this research has been provided by NASA ROSES Grant No. 80NSSC18K0976. We thank David Baker for his help with the XCO_2 data. We also thank Colm Sweeny and Kathryn McKain for their help with aircraft datasets from the NOAA/ESRL Global Greenhouse Gas Reference Network; John Miller, Luciana Gatti, Wouter Peters and Manuel Gloor for their help with the aircraft data from the INPE ObsPack data produc; Steven Wofsy, Kathryn McKain, Colm Sweeny, and Róisín Commane for their help with ATom aircraft datasets; and Debra Wunch for her help with the TCCON datasets. The inverse modeling and data analysis were performed on the NASA Pleiades Supercomputer.

ORCID iDs

Zichong Chen https://orcid.org/0000-0003-2779-1554
Junjie Liu https://orcid.org/0000-0002-7184-6594
Shilong Piao https://orcid.org/0000-0001-8057-2292
Atul K Jain https://orcid.org/0000-0002-4051-3228
Etsushi Kato https://orcid.org/0000-0001-8814-804X
Danica L Lombardozzi https://orcid.org/0000-0003-3557-7929
Joe R Melton https://orcid.org/0000-0002-9414-064X
Hanqin Tian https://orcid.org/0000-0002-1806-4091

References

Ahlström A *et al* 2015 The dominant role of semi-arid ecosystems in the trend and variability of the land CO_2 sink *Science* **348** 895–9

Baker D F *et al* 2006 TransCom 3 inversion intercomparison: impact of transport model errors on the interannual variability of regional CO_2 fluxes, 1988–2003 *Glob. Biogeochem. Cycles* **20** 1

Baldocchi D *et al* 2001 FLUXNET: a new tool to study the temporal and spatial variability of ecosystem-scale carbon dioxide, water vapor, and energy flux densities *Bull. Am. Meteorol. Soc.* **82** 2415–34

Barford C C, Wofsy S C, Goulden M L, Munger J W, Pyle E H, Urbanski S P, Hutyra L, Saleska S R, Fitzjarrald D and Moore K 2001 Factors controlling long-and short-term sequestration of atmospheric CO_2 in a mid-latitude forest *Science* **294** 1688–91

Basu S, Baker D F, Chevallier F, Patra P K, Liu J J and Miller J B 2018 The impact of transport model differences on CO_2 surface flux estimates from OCO-2 retrievals of column average CO_2 *Atmos. Chem. Phys.* **18** 7189–215

Beer C *et al* 2010 Terrestrial gross carbon dioxide uptake: global distribution and covariation with climate *Science* **329** 834–38

Belshe E F, Schuur E A G and Bolker B M 2013 Tundra ecosystems observed to be CO_2 sources due to differential amplification of the carbon cycle *Ecol. Lett.* **16** 1307–15

Bousquet P, Peylin P, Ciais P, Le Quéré C, Friedlingstein P and Tans P P 2000 Regional changes in carbon dioxide fluxes of land and oceans since 1980 *Science* **290** 1342–6

Brix H, Menemenlis D, Hill C, Dutkiewicz S, Jahn O, Wang D, Bowman K and Zhang H 2015 Using Green's Functions to initialize and adjust a global, eddying ocean biogeochemistry general circulation model *Ocean Modell.* **95** 1–14

Bruhwiler L M P, Michalak A M and Tans P P 2011 Spatial and temporal resolution of carbon flux estimates for 1983-2002 *Biogeosciences* **8** 1309–31

Byrne B *et al* 2020 Improved constraints on northern extratropical CO_2 fluxes obtained by combining surface-based and space-based atmospheric CO_2 measurements *J. Geophys. Res. Atmos.* **125** 15

Byrne B, Jones D B, Strong K, Polavarapu S M, Harper A B, Baker D F and Maksyutov S 2019 On what scales can GOSAT flux inversions constrain anomalies in terrestrial ecosystems? *Atmos. Chem. Phys.* **19** 13017–35

Carroll D *et al* 2020 The ECCO-darwin data-assimilative global ocean biogeochemistry model: estimates of seasonal to multi-decadal surface ocean pCO_2 and air-sea CO_2 flux *J. Adv. Model. Earth Syst.* **12** 10

Chatterjee A, Gierach M M, Sutton A J, Feely R A, Crisp D, Eldering A, Gunson M R, O'Dell C W, Stephens B B and Schimel D S 2017 Influence of El Niño on atmospheric CO_2 over the tropical Pacific Ocean: Findings from NASA's OCO-2 mission *Science* **358** eaam5776

Chevallier F, Bréon F M and Rayner P J 2007 Contribution of the Orbiting Carbon Observatory to the estimation of CO_2 sources and sinks: theoretical study in a variational data assimilation framework *J. Geophys. Res. Atmos.* **112** D9

Chevallier F, Remaud M, O'Dell C W, Baker D, Peylin P and Cozic A 2019 Objective 4.1 evaluation of surface-and satellite-driven carbon dioxide atmospheric inversions *Atmos. Chem. Phys.* **19** 14233–51

Cox PM, Pearson D, Booth B B, Friedlingstein P, Huntingford C, Jones C D and Luke C M 2013 Sensitivity of tropical carbon to climate change constrained by carbon dioxide variability *Nature* **494** 341–44

Crowell S *et al* 2019 The 2015–2016 carbon cycle as seen from OCO-2 and the global *in situ* network *Atmos. Chem. Phys.* **19** 9797–831

Deng F *et al* 2014 Inferring regional sources and sinks of atmospheric CO_2 from GOSAT XCO_2 data *ACP* **14** 3703–27

Eldering A *et al* 2017 The Orbiting Carbon Observatory-2 early science investigations of regional carbon dioxide fluxes *Science* **358** 6360

Fang Y and Michalak A M 2015 Atmospheric observations inform CO_2 flux responses to enviroclimatic drivers *Global Biogeochem. Cycles*. **29** 555–66

Friedlingstein P *et al* 2019 Global carbon budget 2019 *Earth Syst. Sci. Data* **11** 1783–838

Friedlingstein P, Meinshausen M, Arora V K, Jones C D, Anav A, Liddicoat S K and Knutti R 2014 Uncertainties in CMIP5 climate projections due to carbon cycle feedbacks *J. Clim.* **27** 511–26

Giglio L, Randerson J T and van der Werf G R 2013 Analysis of daily, monthly, and annual burned area using the fourth-generation global fire emissions database (GFED4) *J. Geophys. Res. Biogeosci.* **118** 317–28

Gourdji S M *et al* 2012 North American CO_2 exchange: inter-comparison of modeled estimates with results from a fine-scale atmospheric inversion *Biogeosciences* **9** 457–75

Gourdji S M, Mueller K L, Schaefer K and Michalak A M 2008 Global monthly averaged CO_2 fluxes recovered using a geostatistical inverse modeling approach: 2. Results including auxiliary environmental data *J. Geophys. Res. Atmos.* **113** D21

Guerlet S, Basu S, Butz A, Krol M, Hahne P, Houweling S, Hasekamp O P and Aben I 2013 Reduced carbon uptake during the 2010 Northern Hemisphere summer from GOSAT *Geophys. Res. Lett.* **40** 2378–83

Gurney K *et al* 2008 Interannual variations in continental-scale net carbon exchange and sensitivity to observing networks estimated from atmospheric CO2 inversions for the period 1980 to 2005 *Global Biogeo. Cycles* **22** 3

Gurney K R *et al* 2003 TransCom 3 CO_2 inversion intercomparison: 1. Annual mean control results and sensitivity to transport and prior flux information *Tellus* B **55** 555–79

Harris I P D J, Jones P D, Osborn T J and Lister D H 2014 Updated high-resolution grids of monthly climatic observations–the CRU TS3. 10 dataset *Int. J. Climatol.* **34** 623–42

Harris I, Osborn T J, Jones P and Lister D 2020 Version 4 of the CRU TS monthly high-resolution gridded multivariate climate dataset *Sci. Data* **7** 1–18

Henze D K, Hakami A and Seinfeld J H 2007 Development of the adjoint of GEOS-chem *Atmos. Chem. Phys.* **7** 9

Hoffman F M *et al* 2014 Causes and implications of persistent atmospheric carbon dioxide biases in Earth System Models *J. Geophys. Res. Biogeosci.* **119** 141–62

Houweling S, Breon F M, Aben I, Rödenbeck C, Gloor M, Heimann M and Ciais P 2004 Inverse modeling of CO_2 sources and sinks using satellite data: a synthetic inter-comparison of measurement techniques and their performance as a function of space and time *Atmos. Chem. Phys.* **4** 523–38

Hu L *et al* 2019 Enhanced North American carbon uptake associated with El Niño *Sci. Adv.* **5** eaaw0076

Humphrey V, Zscheischler J, Ciais P, Gudmundsson L, Sitch S and Seneviratne S I 2018 Sensitivity of atmospheric CO_2 growth rate to observed changes in terrestrial water storage *Nature* **560** 628–31

Huntzinger D N *et al* 2017 Uncertainty in the response of terrestrial carbon sink to environmental drivers undermines carbon-climate feedback predictions *Sci. Rep.* **7** 1–8

Jensen R, Herbst M and Friborg T 2017 Direct and indirect controls of the interannual variability in atmospheric CO_2 exchange of three contrasting ecosystems in Denmark *Agric. For. Meteorol.* **233** 12–31

Jiménez-Muñoz J C, Mattar C, Barichivich J, Santamaría-Artigas A, Takahashi K, Malhi Y, Sobrino J A and Van Der Schrier G 2016 Record-breaking warming and extreme drought in the Amazon rainforest during the course of El Niño 2015–2016 *Sci. Rep.* **6** 1–7

Jung M *et al* 2011 Global patterns of land-atmosphere fluxes of carbon dioxide, latent heat, and sensible heat derived from eddy covariance, satellite, and meteorological observations *J. Geophys. Res. Biogeosci.* **116** G3

Jung M *et al* 2017 Compensatory water effects link yearly global land CO_2 sink changes to temperature *Nature* **541** 516–20

Jung M *et al* 2020 Scaling carbon fluxes from eddy covariance sites to globe: synthesis and evaluation of the FLUXCOM approach *Biogeosciences* **17** 1343–65

Kass R E and Raftery A E 1995 Bayes factors *J. Am. Stat. 266 Assoc.* **90** 773–95

Keppel-Aleks G, Wolf A S, Mu M, Doney S C, Morton D C, Kasibhatla P S, Miller J B, Dlugokencky E J and Randerson J T 2014 Separating the influence of temperature, drought, and fire on interannual variability in atmospheric CO_2 *Glob. Biogeochem. Cycles* **28** 1295–310

Kobayashi S *et al* 2015 The JRA-55 reanalysis: general specifications and basic characteristics *J. Meteorol. Soc. Japan. Ser.* II **93** 5–48

Le Quéré C *et al* 2018 Global carbon budget 2018 *Earth Syst. Sci. Data* **10** 2141–94

Liu J *et al* 2017 Contrasting carbon cycle responses of the tropical continents to the 2015–2016 El Niño *Science* **358** 6360

Liu J *et al* 2021 Carbon monitoring system flux net biosphere exchange 2020 (CMS-flux NBE 2020) *Earth Syst. Sci. Data* **13** 299–330

Liu J, Bowman K, Parazoo N C, Bloom A A, Wunch D, Jiang Z, Gurney K R and Schimel D 2018 Detecting drought impact on terrestrial biosphere carbon fluxes over contiguous US with satellite observations *Environ. Res. Lett.* **13** 095003

Mahadevan P, Wofsy S C, Matross D M, Xiao X, Dunn A L, Lin J C, Gerbig C, Munger J W, Chow V Y and Gottlieb E W 2008 A satellite-based biosphere parameterization for net ecosystem CO_2 exchange: Vegetation Photosynthesis and Respiration Model (VPRM) *Glob. Biogeochem. Cycles* **22** 2

Medvigy D, Wofsy S C, Munger J W and Moorcroft P R 2010 Responses of terrestrial ecosystems and carbon budgets to current and future environmental variability *Proc. Natl Acad. Sci.* **107** 8275–80

Michalak A M, Bruhwiler L and Tans P P 2004 A geostatistical approach to surface flux estimation of atmospheric trace gases *J. Geophys. Res. Atmos.* **109** D14

Miller S M *et al* 2013 Anthropogenic emissions of methane in the United States *Proc. Natl Acad. Sci.* **110** 20018–22

Miller S M *et al* 2016 A multiyear estimate of methane fluxes in Alaska from CARVE atmospheric observations *Glob. Biogeochem. Cycles* **30** 1441–53

Miller S M and Michalak A M 2020 The impact of improved satellite retrievals on estimates of biospheric carbon balance *Atmos. Chem. Phys.* **20** 323–31

Miller S M, Michalak A M, Yadav V and Tadić J M 2018 Characterizing biospheric carbon balance using CO_2 observations from the OCO-2 satellite *Atmos. Chem. Phys.* **18** 6785–99

Miller S M, Saibaba A K, Trudeau M E, Mountain M E and Andrews A E 2020 Geostatistical inverse modeling with very large datasets: an example from the Orbiting Carbon Observatory–2 (OCO–2) satellite *Geosci. Model. Dev.* **13** 1771–85

Oda T, Maksyutov S and Andres R J 2018 The Open-source Data Inventory for Anthropogenic CO_2, version 2016 (ODIAC2016): a global monthly fossil fuel CO_2 gridded emissions data product for tracer transport simulations and surface flux inversions *Earth Syst. Sci. Data* **10** 87–107

Olson D M et al 2001 Terrestrial ecoregions of the world: a new map of life on earth: a new global map of terrestrial ecoregions provides an innovative tool for conserving biodiversity *BioScience* **51** 933–8

Palmer P I, Feng L, Baker D, Chevallier F, Bösch H and Somkuti P 2019 Net carbon emissions from African biosphere dominate pan-tropical atmospheric CO_2 signal *Nat. Commun.* **10** 1–9

Peylin P et al 2013 Global atmospheric carbon budget: results from an ensemble of atmospheric CO_2 inversions *Biogeosciences* **10** 6699–720

Peylin P, Bosquet P, Le Quere C, Sitch S, Friedlingstein P, McKinley G, Gruber N, Rayner P and Ciais P 2005 Multiple constraints on regional CO_2 flux variations over land and oceans *Glob. Biogeochem. Cycles* **19** 1

Piao S et al 2013 Evaluation of terrestrial carbon cycle models for their response to climate variability and to CO2 *Glob Change Biol.* **19** 2117–32

Piao S, Wang X, Wang K, Li X, Bastos A, Canadell J G, Ciais P, Friedlingstein P and Sitch S 2020 Interannual variation of terrestrial carbon cycle: issues and perspectives *Glob. Change Biol.* **26** 300–18

Raftery A E 1995 Bayesian model selection in social research *Sociol. Methodol.* **4** 111–63

Raich J W, Rastetter E B, Melillo J M, Kicklighter D W, Steudler P A, Peterson B J, Grace A L, Moore B III and Vorosmarty C J 1991 Potential net primary productivity in South America: application of a global model *Ecol. Appl.* **1** 399–429

Rienecker M M et al 2011 MERRA: NASA's modern-era retrospective analysis for research and applications *J. Clim.* **24** 3624–48

Rödenbeck C, Houweling S, Gloor M and Heimann M 2003 CO_2 flux history 1982–2001 inferred from atmospheric data using a global inversion of atmospheric transport *Atmos. Chem. Phys.* **3** 1919–64

Saibaba A K and Kitanidis P K 2015 Fast computation of uncertainty quantification measures in the geostatistical approach to solve inverse problems *Adv. Water Resour.* **82** 124–38

Schwalm C R, Black T A, Morgenstern K and Humphreys E R 2007 A method for deriving net primary productivity and component respiratory fluxes from tower-based eddy covariance data: a case study using a 17-year data record from a Douglas-fir chronosequence *Glob. Change Biol.* **13** 370–85

Shiga Y P, Michalak A M, Fang Y, Schaefer K, Andrews A E, Huntzinger D H, Schwalm C R, Thoning K and Wei Y 2018 Forests dominate the interannual variability of the North American carbon sink *Environ. Res. Lett.* **13** 084015

Sitch S et al 2015 Recent trends and drivers of regional sources and sinks of carbon dioxide *Biogeosciences* **12** 653–79

Suyker A E and Verma S B 2001 Year-round observations of the net ecosystem exchange of carbon dioxide in a native tallgrass prairie *Glob. Change Biol.* **7** 279–89

Tarnocai C, Canadell J G, Schuur E A, Kuhry P, Mazhitova G and Zimov S 2009 Soil organic carbon pools in the northern circumpolar permafrost region *Glob. Biogeochem. Cycles* **23** 2

Teluguntla P et al 2015 Global cropland area database (GCAD) derived from remote sensing in support of food security in the twenty-first century: current achievements and future possibilities *Land Resources: Monitoring, Modelling, and Mapping, Remote Sensing Handbook 1* (Boca Raton, FL: CRC Press) (https://doi.org/10.1201/b19322)

Thenkabail P S, Hanjra M A, Dheeravath V and Gumma M 2011 Global croplands and their water use from remote sensing and nonremote sensing perspectives *Advances in Environmental Remote Sensing* (Boca Raton, FL: CRC Press) pp 383–419

Tramontana G et al 2016 Predicting carbon dioxide and energy fluxes across global FLUXNET sites with regression algorithms *Biogeosciences* **13** 4291–313

Wang X et al 2014 A two-fold increase of carbon cycle sensitivity to tropical temperature variations *Nature* **506** 212–5

Wunch D et al 2011 A method for evaluating bias in global measurements of CO_2 total columns from space *Atmos. Chem. Phys.* **11** 12317–337

Yokota T, Yoshida Y, Eguchi N, Ota Y, Tanaka T, Watanabe H and Maksyutov S 2009 Global concentrations of CO_2 and CH_4 retrieved from GOSAT: first preliminary results *Sola* **5** 160–3

Zhao M and Running S W 2010 Drought-induced reduction in global terrestrial net primary production from 2000 through 2009 *Science* **329** 940–3